

Rev. **149**, 257 (1966); **171**, 378 (1968).

¹⁴H. Watanabe, Progr. Theoret. Phys. (Kyoto) **18**, 405 (1957).

¹⁵M. Blume and R. Orbach, Phys. Rev. **127**, 1587 (1962).

¹⁶H. Walther, Z. Physik **170**, 507 (1962).

¹⁷R. M. Sternheimer, Phys. Rev. **146**, 140 (1966).

¹⁸The lattice summations over $(3 \cos^2 \theta - 1)/r^3$ have

been carried out with a computer program employing the Ewald-Kornfeld method.

¹⁹B. O. Loopstra, B. van Laar, and D. J. Breed, Phys. Letters **26A**, 526 (1968); **27A**, 188 (1968).

²⁰D. J. Breed, Physica **37**, 35 (1967).

²¹M. Rubenstein and V. J. Folen, Phys. Letters **28A**, 108 (1968); V. J. Folen, J. Appl. Phys. **40**, 1370 (1969).

PHYSICAL REVIEW B

VOLUME 2, NUMBER 5

1 SEPTEMBER 1970

Iron-Arsenic Associates in ZnSe^\dagger

R. K. Watts

Texas Instruments Incorporated, Dallas, Texas

(Received 13 April 1970)

Electron paramagnetic resonance of Fe^{3+} in the strong trigonal field of a nearest-neighbor substitutional arsenic in ZnSe is reported. Superhyperfine structure is observed from the four nearest neighbors — one arsenic and three seleniums. The parameters appearing in an effective spin Hamiltonian with $S = \frac{1}{2}$ are $g_{\parallel}^e = 2.0238$, $g_{\perp}^e = 6.168$, $A(\text{Fe}^{57}) = 6.2 \times 10^{-4} \text{ cm}^{-1}$, $B(\text{Fe}^{57}) = 16.8 \times 10^{-4} \text{ cm}^{-1}$, $K_{\parallel}(\text{As}^{75}) = 8.71 \times 10^{-4} \text{ cm}^{-1}$, and $K_{\perp}(\text{As}^{75}) = 16.20 \times 10^{-4} \text{ cm}^{-1}$.

I. INTRODUCTION

Impurity associates are rather common in the II-VI compounds.^{1,2} Fe^{3+} has been shown to associate in them with copper, silver, or lithium at a next-nearest-neighbor lattice site, the magnetic properties being those of $(3d)^5 S$ in a field of C_s symmetry.² This paper reports magnetic resonance of Fe^{3+} in the strong trigonal field produced by a nearest-neighbor arsenic associate in ZnSe .

II. MEASUREMENTS

ZnSe was compounded by allowing elemental zinc to react with H_2Se gas. Small amounts of arsenic and iron were added, and single crystals were grown from the melt in a sealed ampoule by a gradient-freeze technique.³ Resonances were observed at 1.3 K with a superheterodyne spectrometer operating at 9 GHz. The crystals were mounted on the end of a quartz light pipe which extended along the axis of the right circular cylindrical cavity. The crystals could be irradiated through the light pipe with light from a 1.5-kW mercury-arc lamp and monochromator. The magnetic field was rotated in a $\{110\}$ crystallographic plane.

In all samples, a weak signal consisting of four lines and smaller satellites with g factor 2 for the magnetic field along a $\langle 111 \rangle$ axis and 6 for the field perpendicular to the axis was observed. See Figs. 1 and 2. The signal is much weaker than that due to unassociated arsenic⁴ and is observed also in samples not intentionally doped with iron. Iron is a common contaminant in all II-VI compounds. Iron doping increases the strength of the signal.

Doping with iron isotopically enriched to 98% Fe^{57} with nuclear spin $\frac{1}{2}$ causes a doubling of the number of spectral lines, as shown in Figs. 3 and 4. In this manner Fe^{3+} is identified as the paramagnetic ion. A strong axial electric field is known to produce the observed g factors. The four equally intense lines of the spectra are interpreted to arise from the hyperfine interaction with an As ion on the symmetry axis; in fact, this ion defines this axis. The angular dependence of the spectrum is described by the effective spin Hamiltonian⁵

$$\begin{aligned} \mathcal{H}^e = & g_{\parallel}^e \beta H_z S_z + g_{\perp}^e \beta (H_x S_x + H_y S_y) + A(\text{Fe}^{57}) I_z \\ & \times (\text{Fe}) S_z + B(\text{Fe}^{57}) [I_x(\text{Fe}) S_x + I_y(\text{Fe}) S_y] \\ & + K_{\parallel}(\text{As}^{75}) I_z(\text{As}) S_z + K_{\perp}(\text{As}^{75}) [I_x(\text{As}) S_x \\ & + I_y(\text{As}) S_y] + \sum_{i=1}^3 \vec{S} \cdot \vec{K}(\text{Se}^{77}) \cdot \vec{I}(\text{Se}), \end{aligned} \quad (1)$$

where

$$g_{\parallel}^e = 2.0238 \pm 0.0005,$$

$$A(\text{Fe}^{57}) = (6.2 \pm 0.2) \times 10^{-4} \text{ cm}^{-1},$$

$$g_{\perp}^e = 6.168 \pm 0.002,$$

$$B(\text{Fe}^{57}) = (16.8 \pm 0.7) \times 10^{-4} \text{ cm}^{-1},$$

$$K_{\parallel}(\text{As}^{75}) = (8.71 \pm 0.15) \times 10^{-4} \text{ cm}^{-1}, \quad S = \frac{1}{2}$$

$$K_{\perp}(\text{As}^{75}) = (16.20 \pm 0.68) \times 10^{-4} \text{ cm}^{-1}, \quad \hat{z} \parallel \langle 111 \rangle.$$

The small satellite lines seen in the figures are interpreted as a superhyperfine spectrum from three selenium nuclei. When the magnetic field is along the $\langle 111 \rangle$ symmetry axis these three nuclei are magnetically equivalent. In this case two satellites about each main line with intensity 0.11 rela-

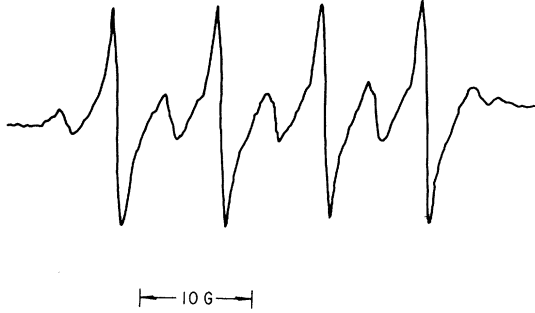


FIG. 1. Spectrum with magnetic field along $\langle 111 \rangle$, showing As^{75} splitting (four strong lines) and Se^{77} splitting (weak satellites).

tive to the main line are to be expected, since Se^{77} with nuclear spin $\frac{1}{2}$ is 7.5% abundant. The observed ratio is indeed 0.11. Since these satellites are well resolved only for the magnetic field direction near $\langle 111 \rangle$, the complete tensor $\overline{\mathbf{K}}$ (Se^{77}) could not be determined. The selenium splitting for $\mathbf{H} \parallel \langle 111 \rangle$ is $(8.9 \pm 0.7) \times 10^{-4} \text{ cm}^{-1}$.

The signal is photosensitive and decreases slightly upon irradiation with light of near-band-gap energy. No resonance due to unassociated Fe^{3+} was observed in the samples, although it is commonly observed in ZnSe not doped with arsenic.

III. DISCUSSION

In a trigonal electric field the levels of $\text{Fe}^{3+} \times (3d)^5 {}^6S$ are split into three doublets. Only if the $M_s = \pm \frac{1}{2}$ doublet is lowest will a resonance be observed in a strong axial field.⁶ Observation of the g factors 2 and 6 with the simple angular dependence of Eq. (1) implies that the splitting of 6S is large compared with the microwave quantum. This type of spectrum (Fe^{3+} in a strong axial field with the $\pm \frac{1}{2}$ doublet lowest) has been observed by other workers, perhaps the best known example being the resonance due to iron in hemoglobin.⁶

In this section the connection between the effective spin Hamiltonian of Eq. (1) and the spin Hamiltonian appropriate to 6S in a trigonal field will be explored. If the hyperfine and superhyperfine terms are omitted, this Hamiltonian is written

$$\mathcal{H} = \beta H (g_{\parallel} \cos \theta S_x + g_{\perp} \sin \theta S_x) + b_2^0 O_2^0 + b_4^0 O_4^0 + b_4^3 O_4^3. \quad (2)$$

$S = \frac{5}{2}$, and the x , y , z axes are taken as $[-1, -1, 2]$, $[1, -1, 0]$, $[1, 1, 1]$; the magnetic field rotates in the x - z plane. θ is the angle between $[111]$ and the magnetic field \mathbf{H} . The crystal field is represented by the last three terms, the relation between the field and the parameters $b_{2,4}^n$ being quite complicated for an S state. The operators O_2^0 , O_4^0 , and

O_4^3 contain components of $\overline{\mathbf{S}}$ and are defined by Hutchings.⁷ The matrix of this Hamiltonian among the six states of $|M_s\rangle$ of 6S is shown in Table I. The new symbols are

$$\begin{aligned} A &= 10b_2^0 + 60b_4^0, & \delta &= g_{\perp} \beta H \sin \theta, \\ B &= -8b_2^0 + 120b_4^0, & h &= \frac{1}{2} (\gamma^2 + 9\delta^2)^{1/2}, \\ C &= -2b_2^0 - 180b_4^0, & a_1 &= [(2h + \gamma)/4h]^{1/2}, \\ \gamma &= g_{\parallel} \beta H \cos \theta, & a_2 &= [(2h - \gamma)/4h]^{1/2}. \end{aligned}$$

The states $|\pm \frac{1}{2}\rangle$ have been rotated to form new states $|\pm\rangle$ defined by

$$|+\rangle = a_1 |\frac{1}{2}\rangle + a_2 |-\frac{1}{2}\rangle, \quad |-\rangle = a_2 |\frac{1}{2}\rangle - a_1 |-\frac{1}{2}\rangle.$$

The effective g factor observed for the ground doublet will be calculated using third-order perturbation theory. The perturbation will be taken as the Zeeman energy and $b_4^3 O_4^3$. $b_2^0 O_2^0$ should be by far the largest term of Eq. (2); $b_4^0 O_4^0$ may be of the same order of magnitude as $b_4^3 O_4^3$, but it appears only in the diagonal elements. The effective- g factor of the perturbed $|\pm\rangle$ doublet is then $(E_+ - E_-)/\beta H$, where E_{\pm} is the energy of a component of the doublet as given by perturbation theory. The result is

$$g^e(\theta) = (g_{\parallel}^2 \cos^2 \theta + 9g_{\perp}^2 \sin^2 \theta)^{1/2} \times \left(1 - \frac{2(g_{\perp} \beta H)^2}{(B - C)^2} F(\theta) - \frac{90(b_4^3)^2}{(B - A)^2} G(\theta) \right), \quad (3)$$

where

$$\begin{aligned} F(\theta) &= \sin^2 \theta \left(\frac{9g_{\perp}^2 \sin^2 \theta - 2g_{\parallel}^2 \cos^2 \theta}{g_{\parallel}^2 \cos^2 \theta + 9g_{\perp}^2 \sin^2 \theta} \right), \\ G(\theta) &= \frac{6g_{\parallel}^2 \cos^2 \theta + 9g_{\perp}^2 \sin^2 \theta}{g_{\parallel}^2 \cos^2 \theta + 9g_{\perp}^2 \sin^2 \theta}. \end{aligned}$$

This derivation is similar to that of Kirkpatrick *et al.*⁸ except that admixture of $|\pm \frac{5}{2}\rangle$ by the off-diagonal part of the crystal-field term is included

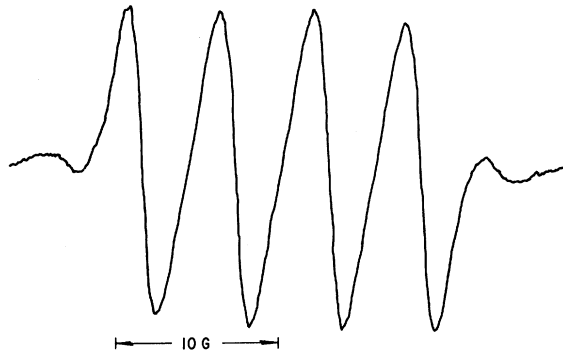


FIG. 2. Spectrum with magnetic field perpendicular to $\langle 111 \rangle$.

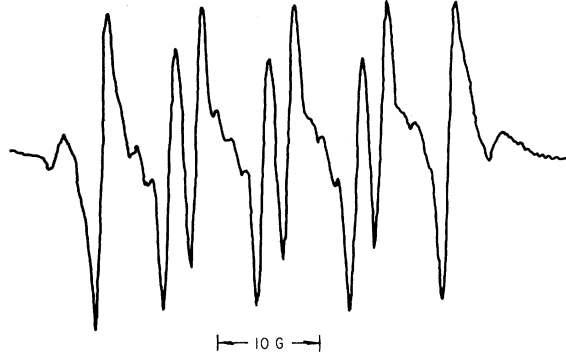


FIG. 3. Spectrum with magnetic field along $\langle 111 \rangle$, iron isotopically enriched to 98% Fe^{57} . Note the doubling of the number of lines caused by the nuclear spin of Fe^{57} .

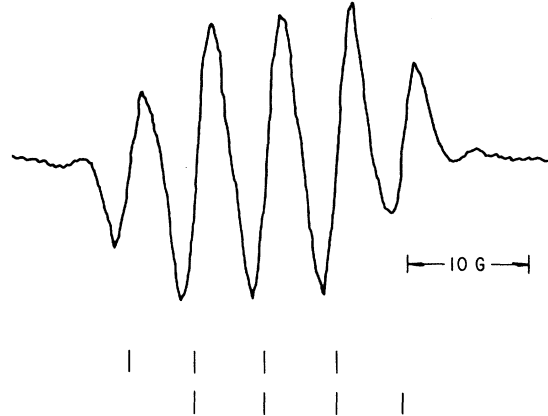


FIG. 4. Spectrum with magnetic field perpendicular to $\langle 111 \rangle$, iron isotopically enriched to 98% Fe^{57} . The vertical lines indicate the doubled As spectrum.

here. [There are typographical errors in their expression for $F(\theta)$, but their expressions for $g^e(0^\circ)$ and $g^e(90^\circ)$ are correct.]

In order that the term containing $F(\theta)$ have no observable effect on the angular dependence of the spectrum, the separation between ground and first excited doublets must be at least about 10 cm^{-1} . The g factors appearing in Eq. (2) are then

$$g_{\parallel} = g_{\parallel}^e = 2.0238 \pm 0.0005, \quad g_{\perp} = \frac{1}{3} g_{\perp}^e = 2.056 \pm 0.001.$$

Study of the spectrum at higher microwave frequencies would be useful, since the term in $F(\theta)$ would be larger. An experiment at 35 GHz was tried, but after the sample had been cut to a small enough size to avoid excessively perturbing the mode of the smaller cavity, the signal from the reduced number of ions was too weak for study.

The positive g shift has been explained by Watanabe⁹ in terms of charge transfer. He has given an approximate formula¹⁰ connecting b_2^0 with $g_{\parallel} - g_{\perp}$:

$$b_2^0 = \frac{1}{30} (g_{\perp} - g_{\parallel}) \zeta_{3d}. \quad (4)$$

If Watanabe's value of 486 cm^{-1} is used for the Fe^{3+} spin-orbit parameter ζ_{3d} , then Eq. (4) predicts a value of 0.52 cm^{-1} for b_2^0 . The zero-field splitting between ground and first excited states is $C - B = 6b_2^0 - 300b_4^0$. If the term in b_4^0 can be neglected compared with $6b_2^0$, this gives a value of 3 cm^{-1}

for the splitting, too small by at least a factor of 3, but of the proper sign.

The model for this center, as shown in Fig. 5, is suggested by the superhyperfine structure. Fe^{3+} substitutes for a zinc with an arsenic ion substitutional for a nearest-neighbor selenium. The most likely charge state of the arsenic is triply negative. This provides charge compensation and leaves the arsenic diamagnetic. The other three nearest-neighbor seleniums cause the observed selenium superhyperfine structure.

The large splitting of the iron levels seems reasonable on this model. For the next-nearest-neighbor iron-copper associate in ZnSe Holton *et al.*² found a splitting of 3.23 cm^{-1} between ground and first excited doublets. For a closer association a larger splitting is to be expected.

ACKNOWLEDGMENTS

I thank W. C. Holton and M. de Wit for reading the manuscript and making helpful comments on it and R. D. Stinedurf for growing the ZnSe crystals.

APPENDIX

The spin Hamiltonian of Eq. (2) is frequently written¹¹ in the form

TABLE I. The matrix of the Hamiltonian, Eq. (2), among the six states $|M_S\rangle$ of 6S .

$ +\rangle$	$ -\rangle$	$ \frac{3}{2}\rangle$	$ -\frac{3}{2}\rangle$	$ \frac{5}{2}\rangle$	$ -\frac{5}{2}\rangle$
$B+h$	0	$\sqrt{2}\delta a_1$	$\sqrt{2}\delta a_2$	$3(\sqrt{10})b_4^3 a_2$	$-3(\sqrt{10})b_4^3 a_1$
0	$B-h$	$\sqrt{2}\delta a_2$	$-\sqrt{2}\delta a_1$	$-3(\sqrt{10})b_4^3 a_1$	$-3(\sqrt{10})b_4^3 a_2$
$\sqrt{2}\delta a_1$	$\sqrt{2}\delta a_2$	$C+\frac{3}{2}\gamma$	0	$\frac{1}{2}(\sqrt{5})\delta$	0
$\sqrt{2}\delta a_2$	$-\sqrt{2}\delta a_1$	0	$C-\frac{3}{2}\gamma$	0	$\frac{1}{2}(\sqrt{5})\delta$
$3(\sqrt{10})b_4^3 a_2$	$-3(\sqrt{10})b_4^3 a_1$	$\frac{1}{2}(\sqrt{5})\delta$	0	$A+\frac{5}{2}\gamma$	0
$-3(\sqrt{10})b_4^3 a_1$	$-3(\sqrt{10})b_4^3 a_2$	0	$\frac{1}{2}(\sqrt{5})\delta$	0	$A-\frac{5}{2}\gamma$

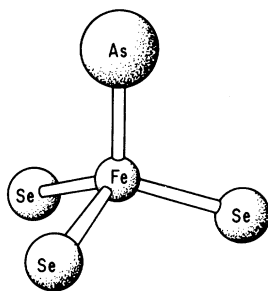


FIG. 5. Model of the center with Fe^{3+} substitutional for Zn^{2+} and As^{3-} substitutional for a nearest Se^{2-} .

$$\begin{aligned} \mathcal{H} = & \beta \vec{H} \cdot \vec{g} \cdot \vec{S} + D[S_z^2 - \frac{1}{3}S(S+1)] + \frac{1}{6}a[S_x^4 + S_y^4 + S_z^4 \\ & - \frac{1}{5}S(S+1)(3S^2 + 3S - 1)] + \frac{1}{180}F[35S_z^4 \\ & - 30S(S+1)S_z^2 + 25S^2 - 6S(S+1) + 3S^2(S+1)^2]. \end{aligned}$$

The ξ , η , ζ axes are parallel to the fourfold cubic axes. The connection between the parameters appearing in the two forms is given by

$$b_2^0 = \frac{1}{3}D, \quad b_4^0 = \frac{1}{180}(F - a), \quad b_4^3 = \frac{1}{9}(a/2),$$

where only the cubic contribution to b_4^3 has been considered.

[†]Research sponsored in part by the Air Force Office of Scientific Research, Contract No. F44620-67-C-0073.

¹R. S. Title, B. L. Crowder, and J. W. Mayo, in *II-VI Semiconducting Compounds*, edited by D. G. Thomas (Benjamin, New York, 1967), p. 1367; J. Schneider, *ibid.*, p. 40; R. K. Watts and W. C. Holton, *Phys. Rev.* **173**, 417 (1968); W. C. Holton, M. de Wit, R. K. Watts, T. L. Estle, and J. Schneider, *J. Phys. Chem. Solids* **30**, 963 (1969).

²W. C. Holton, M. de Wit, T. L. Estle, B. Dischler, and J. Schneider, *Phys. Rev.* **169**, 359 (1968).

³W. C. Holton, R. K. Watts, and R. D. Stinedurf, *J. Crystal Growth* **6**, 97 (1969).

⁴W. C. Holton, A. R. Reinberg, R. K. Watts, and M. de Wit, *J. Luminescence* **1**, 583 (1970).

⁵H. H. Wickman, M. P. Klein, D. A. Singleton, J.

Chem. Phys. **42**, 2113 (1965).

⁶J. E. Bennett, J. F. Gibson, and D. J. E. Ingram, *Proc. Roy. Soc. (London)* **A240**, 67 (1957).

⁷M. T. Hutchings, in *Solid State Physics*, edited by F. Seitz and D. Turnbull (Academic, New York, 1964), Vol. 16, p. 227.

⁸E. S. Kirkpatrick, K. A. Müller, and R. S. Rubins, *Phys. Rev.* **135**, A86, (1964).

⁹H. Watanabe, *J. Phys. Chem. Solids* **25**, 1471 (1964).

¹⁰H. Watanabe, in *II-VI Semiconducting Compounds*, edited by D. G. Thomas (Benjamin, New York, 1967), p. 1381.

¹¹J. Schneider, S. R. Sircar, and A. Räuber, *Z. Naturforsch.* **18A**, 980 (1963).

Electronic Raman Spectrum and Crystal Field of the Terbium Ion in Terbium Aluminum Garnet*

J. A. Koningstein and G. Schaack[†]

Department of Chemistry, Carleton University, Ottawa, Ontario, Canada

(Received 29 September 1969)

Electronic Raman transitions of Tb^{3+} in $\text{Tb}_3\text{Al}_5\text{O}_{12}$ (garnet) within the 7F_6 ground-state components and to the excited states of the 7F_5 components have been observed. From the polarization properties of the Raman transitions, the symmetry of some of the states of the Tb^{3+} ions in this crystal has been determined. A Zeeman-Raman experiment has been performed. Relations between the observed components of the scattering tensors of cubic symmetry and the tensors for transitions of the ions in the orthorhombic site symmetry have been established. Based on these results, the justification of the cubic and tetragonal approximations of the crystal field in this compound is discussed.

I. INTRODUCTION

The study of transitions between electronic states of the $4f$ shell of rare-earth ions in solids by inelastic scattering of light is a relatively new branch of research.¹ The present available extensive knowledge of these states — that is, the energy of the states and the wave functions — has been the result of studies of electric and magnetic dipole

transitions between these states.² However, the observations of Raman transitions of trivalent rare-earth ions in solids occurred, except in one case,³ after the advent of the laser,⁴ and the importance of this new technique with regard to extending the above-mentioned properties may lead to new developments in the application of crystal-field theory.⁵ There are two reasons why these developments may take place. First, the Raman